The Role of Cholesterol in the Activity of Pneumolysin, a Bacterial Protein Toxin

Marcelo Nöllmann,* Robert Gilbert,[†‡] Timothy Mitchell,* Michele Sferrazza,[§] and Olwyn Byron*
*Division of Infection and Immunity, Institute of Biomedical and Life Sciences, University of Glasgow, Glasgow, Scotland, United Kingdom; [†]Division of Structural Biology, Wellcome Trust Centre for Human Genetics, and [‡]Oxford Centre for Molecular Sciences, Central Chemistry Laboratory, University of Oxford, Oxford, United Kingdom; and [§]Department of Physics, University of Surrey, Guildford, United Kingdom

ABSTRACT The mechanism via which pneumolysin (PLY), a toxin and major virulence factor of the bacterium *Streptococcus pneumoniae*, binds to its putative receptor, cholesterol, is still poorly understood. We present results from a series of biophysical studies that shed light on the interaction of PLY with cholesterol in solution and in lipid bilayers. PLY lyses cells whose walls contain cholesterol. Using standard hemolytic assays we have demonstrated that the hemolytic activity of PLY is inhibited by cholesterol, partially by ergosterol but not by lanosterol and that the functional stoichiometry of the cholesterol-PLY complex is 1:1. Tryptophan (Trp) fluorescence data recorded during PLY-cholesterol titration studies confirm this ratio, reveal a significant blue shift in the Trp fluorescence peak with increasing cholesterol concentrations indicative of increasing nonpolarity in the Trp environment, consistent with cholesterol binding by the tryptophans, and provide a measure of the affinity of cholesterol binding: $K_d = 400 \pm 100$ nM. Finally, we have performed specular neutron reflectivity studies to observe the effect of PLY upon lipid bilayer structure.

INTRODUCTION

The study of processes leading to eukaryotic membrane disruption and pore formation is fundamental to gain a comprehensive understanding of cell lysis resulting from bacterial toxins. One such group of toxins is the highly homologous cholesterol-binding (also historically but wrongly referred to as thiol-activated) bacterial protein toxins (CBTs, also known as cholesterol-dependent cytotoxins or CDCs) which are virulence factors of Gram-positive bacteria, and include pneumolysin (PLY), perfringolysin (PFO), listeriolysin (LLO), and streptolysin (SLO) (see Tweten, 1995). PLY is a 53 kDa hemolytic protein toxin that constitutes one of the several potential virulence factors produced by *Streptococcus pneumoniae*, which causes various human diseases such as pneumonia, otitis media, meningitis, and bacteremia (Paton et al., 1993; Canvin et al., 1997).

An atomic structure of PLY is not yet available, although Kelly and Jedrzejas (2000a) recently reported the successful crystallization of PLY complexed with a cholesterol analog. Electron microscopy (Morgan et al., 1994), cryoelectron microscopy (Gilbert et al., 1999b), and homology models (Rossjohn et al., 1998) have provided the only structural information hitherto available. On the basis of its homology with PFO (48% sequence identity and 60% sequence similarity), PLY is thought to be a long rod-shaped molecule comprising four domains with overall dimensions of 110 Å $\times$ 50 Å $\times$ 30 Å. Its secondary structure is mainly composed of β-sheet motifs (Rossjohn et al., 1998), although domain 3 is thought to contain several short α-helices.

The most conserved region of the CBTs is a sequence of 11 amino acids (*ECTGLAWEWWR*, also referred to as the *Trp-rich loop*) at the base of the fourth domain, which is thought to be responsible for membrane binding (Watson et al., 1972). Biological and biophysical studies have shed light on the specific mechanisms used by these toxins to bind to (Jacobs et al., 1998, 1999; Nakamura et al., 1995; Tweten et al., 1991) and further insert into (Palmer et al., 1996; Shepard et al., 1998; Shatursky et al., 1999; Nakamura et al., 1995; Heuck et al., 2000) cell membranes, and on their cooperative self-organizing oligomerization (Morgan et al., 1995, 1994) fostering pore formation and subsequent cell lysis (Paton et al., 1993).

Two distinguishable but dependent processes, membrane binding and protein oligomerization, collaborate in the pore-formation process. A mechanism for CBT pore formation consistent with accumulated biochemical and biophysical data was proposed by Gilbert (2002) as follows: soluble monomeric toxin binds to the membrane in a cholesterol-dependent manner via the carboxy-terminal fourth domain. Dimerization of bound toxin is the first stage of either uni- or bidirectional oligomerization which can terminate with as many as 50 monomers forming a large ($\approx$350 Å diameter; Morgan et al., 1994) assembly on the cell surface. The PFO prepore inserts into the membrane in a concerted action when two groups of three small α-helices in domain 3 refold to form two β-hairpins capable of forming the lumen of the pore (Hotze et al., 2002). An alternative model for PFO pore formation has been proposed by Rossjohn et al. (1997), in which toxin insertion precedes pore formation. As yet, equivalent data for PLY remain to be acquired.

The inhibition of thiol-activated pore-forming toxins by preincubation with cholesterol reported in the early 1970s by Watson et al. (1972) provided the first evidence that this

Submitted May 29, 2003, and accepted for publication October 10, 2003.

Address reprint requests to Olwyn Byron, Tel.: 44-0-141-330-3752; Fax: 44-0-141-330-4600; E-mail: o.byron@bio.gla.ac.uk.

0006-3495/04/05/3141/11 $2.00

major constituent of eukaryotic cell membranes could be the receptor for this family of toxins (see Duncan and Schlegel, 1975; Prigent and Alouf, 1976; Johnson et al., 1980, or for a more recent article, Morgan et al., 1996). Preincubation with cholesterol was thought to saturate all available binding sites on the toxin, thwarting the further binding of the protein with the cell membrane. That these CBTs do not attack bacterial cell membranes (which contain ergosterol rather than cholesterol in their membranes) was also evidence in support of the above hypothesis. More recent studies focusing on the effects triggered by membrane binding (for example, monitoring cytokine expression and release of IL-1) of LLO preincubated with cholesterol have suggested that membrane association of the protein toxin-cholesterol complex takes place but without any sign of cell lysis or pore formation (Nishibori et al., 1996; Yoshikawa et al., 1993; Sibelius et al., 1996). Further evidence supporting these results has been provided by Jacobs et al. (1998), who used immunoblot analysis and flow cytometry to study the binding and pore formation of LLO, demonstrating that preincubation of LLO with cholesterol does not influence the binding of this toxin to the cell membrane, but does affect the polymerization process leading to pore formation. In this article we present new results that further clarify the role played by cholesterol as the putative receptor for cholesterol-binding toxins in general and PLY in particular.

The lack of hydrophobic patches identifiable on either the PLY homology model surface or its domain interfaces was at first surprising, since they constitute a common mechanism for membrane disruption (Tweten, 1995; Alouf and Geoffroy, 1991). Instead a novel mechanism was proposed by Rossjohn and colleagues (Rossjohn et al., 1997, 1998; Gilbert et al., 1999b). According to this mechanism, binding to cholesterol displaces the Trp-rich motif from its original position, which results in the formation of a hydrophobic dagger that inserts into the membrane and may contribute to membrane disruption. Alternatively, it has been suggested that monomeric PLY would just sit on the cell membrane (Ramachandran et al., 2002), triggering its destabilization, and that the cooperative effect of further protein oligomerization may finally foster membrane disruption, after pore formation (Bonev et al., 2001).

Several fluorescence studies with liposomes as model membranes have been carried out in order to gain understanding of the binding-insertion mechanisms used by CBTs. Nakamura et al. (1995) found that the tryptophan fluorescence intensity of PFO changed when the toxin inserted into cholesterol-containing liposomes. In a more recent article, Shepard et al. (1998) have monitored the changes in the PFO Trp fluorescence maximum upon membrane binding and insertion, and have found a fluorescence blue shift which indicates (Vivian and Callis, 2001) that the environments of the Trp residues becomes more nonpolar. If the overall Trp fluorescence emission is attributed to the Trp residues in the Trp-rich loop, this indicates that this loop is moving from a polar to a hydrophobic environment upon binding/insertion. In addition, Heuck et al. (2000) have studied the changes in PFO Trp fluorescence upon binding to cholesterol-containing liposomes as a function of cholesterol concentration. Based on these measurements, the authors propose a pore-formation mechanism which comprises the following steps: 1), domain 4 superficially binds to the membrane and finds its final position without being deeply embedded into the membrane core; 2), in response to the binding of domain 4, domain 3 undergoes a conformational change and inserts into the membrane; and 3), it then acts to foster oligomerization and further pore-formation. Interactions of domains 3 and 4 with the membrane are reported to be strongly dependent on the concentration of cholesterol in the liposome membrane.

More recently, Kelly and Jedrzejas (2000b) investigated the characteristics of binding between a water-soluble cholesterol analog (ws-chol) and PLY in solution, and found differences in the CD spectra, hydrodynamic properties, and Trp fluorescence of the ws-chol-PLY complex with respect to monomeric PLY. However, the interaction of ws-chol with PLY may be completely different from that of true cholesterol because of significant structural differences (Fig. 1) between the two ligands. Therefore the results of Kelly and Jedrzejas might not be truly relevant to the understanding of the role of cholesterol in CBT pore-formation mechanisms.

Small-angle neutron scattering data have provided an insight into the pore-formation mechanism of PLY (Gilbert et al., 1999a, 1998). Different components of biological systems possess different neutron scattering lengths, which depend on their atomic composition and volume. The scattering lengths of hydrogen and deuterium are very dissimilar, 6.7 fm and -3.7 fm, respectively. By mixing appropriate ratios of hydrogenated (light) and deuterated (heavy) water, it is possible to match the scattering lengths of different components of a biological system, making them ''invisible'' and enabling an experiment to focus on visible components (see e.g., Byron and Gilbert, 2000). In the experiments performed by Gilbert and co-workers, PLY was chemically derivatized with dithionitrobenzoic acid to covalently label the only cysteine residue in PLY (Cys-428) with a thionitrobenzoic (TNB) acid moiety. PLY-TNB retained the ability to bind to the phospholipid membrane but lacked the ability to oligomerize (Gilbert et al., 1999a), confirming that the processes of cell binding and oligomerization are functionally separate. Derivatization was reversed by the addition of dithiothreitol (DTT) in situ, after which partial protein activity was restored.

The surface of phosphatidylcholine/cholesterol/dicetyl phosphate liposomes has been shown to thicken after addition of PLY-TNB, which has been interpreted as being due to the binding of PLY-TNB monomers to the liposomal surface without forming any pores (Gilbert et al., 1999a). In

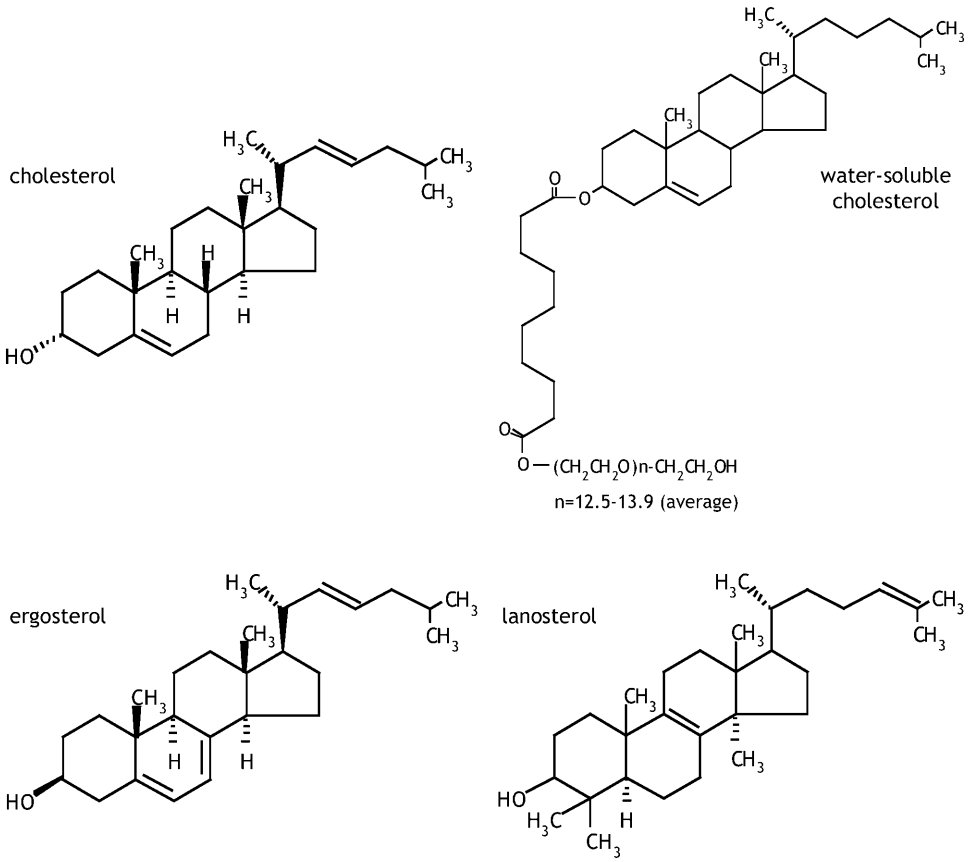

FIGURE 1 Structures of cholesterol (the cell-surface receptor for pneumolysin), water-soluble cholesterol, ergosterol, and lanosterol molecules.

contrast, the surface of the liposomes thins when attacked by wild-type (WT) PLY, clear evidence of the pore-formation process taking place. The same thinning was observed after addition of DTT to the sample containing liposomes and PLY-TNB, which demonstrated that the thinning was due to pore formation.

MATERIALS AND METHODS

Materials

Phosphatidylcholine (L-α-phosphatidylcholine from frozen egg yolk, purity by TLC: 99%), dicetyl phosphate, cholesterol, ergosterol, lanosterol, and deuterated water (99.9%) were from Sigma. Deuterated cholesterol (24, 24, 25, 25, 26, and 26-D, 95% deuteration) was from Medical Isotopes (Pelham, NH).

Protein expression, purification, and derivatization

PLY was overexpressed in M15 *E. coli*, using a protocol described elsewhere (Gilbert et al., 1998). Protein purification was performed using hydrophobic and ion-exchange columns on a BioCAD perfusion chromatography workstation (Applied Biosystems). Protein purity (>90%) was assessed by SDS PAGE under reducing conditions. The protein was immediately derivatized after purification using Ellman's reaction in which the only free thiol group in PLY at residue C428 is reacted with dithio(bis)nitrobenzoate to produce pneumolysin-thionitrobenzoate, i.e., PLY-TNB (Gilbert et al., 1998).

Liposome manufacture

Liposomes were prepared using a modification of a procedure described earlier (Gilbert et al., 1998). The liposome mixture (phosphatidylcholine/*sterol*/dicetyl phosphate in a molar ratio 10:*x*:1, where *sterol* is either cholesterol or ergosterol and *x* ranges from 0 to 10) was firstly dissolved in a 1:1 (v/v) chloroform/methanol solution. For neutron reflectivity experiments the molar concentration of cholesterol was the same as that of phosphatidylcholine (i.e., *x* was 10). The absolute molar concentration was such that when dissolved in the final volume of aqueous buffer the solution had a total lipid plus cholesterol molarity of 2 mM. The solution was then dried under nitrogen and resuspended in CHB (50 mM NaH_2PO_4 and 200 mM NaCl, pH 4.8). Finally, the lipid solution was vortexed, sonicated (using a bath sonicator at 45°C for 45 min), repeatedly extruded through 0.2 μm filters and centrifuged for 20 min at 3000 *g*. The liposomes were determined to be spherical with an average size of 50 $\pm$ 10 nm by dynamic light scattering using a DynaPro MS800 single-angle detector instrument (Protein Solutions, Lakewood, NJ). Two different types of cholesterol were employed: standard hydrogenated and deuterated cholesterol (24, 24, 25, 25, 26, and 26-D; from Medical Isotopes, Pelham, NH).

Activity assays

PLY activity was assayed using a hemolytic assay (Walker et al., 1987). 50 ml of PBS buffer (125 mM NaCl, 1.5 mM KH_2PO_4, 8 mM Na_2HPO_4 and 2.5 mM KCl, pH 7.6) were loaded into the cells of a 96-well plate.

Cholesterol/PLY solutions were prepared using a 7 μM PLY stock solution in PBS and stock cholesterol, ergosterol and lanosterol solutions in 100% ethanol. The samples were then vortexed and incubated for 5 min. Samples to be assayed were loaded into the first cell of each row and double-diluted across the plate so that the first column contained the more concentrated sample and the last column contained the most dilute. 1 ml of whole sheep blood was centrifuged and its pellet resuspended in 20 ml of PBS buffer and then loaded (50 μl) into each well. Lastly, the plate was incubated at 37°C for 30 min. The red blood cells that are not lysed sink to the bottom of the well and form a clear red dot in an otherwise transparent solution. On the other hand, the lysed cells release their hemoglobin, giving the solution a red color that provides a way of monitoring the protein lysing activity. Hemolytic units (HU) were expressed as the reciprocal of the dilution at which 50% lysis was observed.

Fluorescence

Fluorescence spectra were taken at room temperature (20°C) using a SpectraMax (Molecular Devices, Sunnyvale, CA) fluorimeter. Tryptophan residues were excited at a wavelength of 290 nm, and their fluorescence emission scanned from 300 to 520 nm. The fluorescence emission intensity was taken from the maximum of the spectra recorded for the different cholesterol/PLY ratios (between 350 and 340 nm). The protein was used at an initial concentration of 7 μM in PBS.

Neutron reflectivity experiments

Specular neutron reflectivity studies were performed on the SURF reflectometer at the ISIS spallation neutron source, Rutherford Appleton Laboratory (Didcot, UK). A standard instrument configuration was used and data collection and reduction proceeded as described by Penfold (1991) and Penfold et al. (1987). Samples were housed in a solid/liquid cell (fully described by Marsh et al., 1999). The silicon block through which the neutrons travel is a single polished crystal of size 25 mm $\times$ 51 mm $\times$ 127 mm, presenting a [111] plane to the adsorbed liquid. The silicon block surface facing down into the trough was cleaned by immersion into a mixture of 90% (v/v) sulphuric acid and 10% hydrogen peroxide heated to 100°C for 10 min. This procedure generated an extremely hydrophilic SiO_2 layer on the surface of the block that was assessed by its ability to retain a layer of water when inclined vertically.

Solvents of three different neutron scattering length densities (or contrasts) were used. The contrast is the result of the large difference in neutron scattering length density between deuterium and hydrogen (see above). Using a combination of deuterated and protonated solvent, different contrasts can be obtained that give different reflectivity profiles whereas the interface remains unchanged. The contrast solvents used were: PBS buffer made with 100% D_20; PBS buffer made with 100% H_20; and PBS buffer made with 42.3% (w/v) D_20, which has the same neutron scattering length density as the silicon substrate. The calculated scattering length densities of the three solvents are 6.35 $\times$ 10^{-6} Å^{-2}, -0.56 $\times$ 10^{-6} Å^{-2}, and 2.07 $\times$ 10^{-6} Å^{-2}, respectively.

RESULTS

The hemolytic activity of PLY is inhibited by cholesterol, partially by ergosterol but not by lanosterol

Cholesterol and coprostenol have been shown to be equally effective in inhibiting toxin activity, whereas cholestanol and coprostenol are slightly less efficient (Smyth and Duncan, 1978). The presence of an α-OH group on the sterol C-3 atom (Fig. 1) is essential for its inhibiting activity, whereas other compositional changes have been shown to reduce its effectiveness (see Smyth and Duncan, 1978). The structure of ergosterol is only slightly different from that of cholesterol (the out-of-plane angle of α-OH, and a hydrogen atom missing from C-8) whereas lanosterol differs more in its ring structure. More different still is water-soluble cholesterol (Kelly and Jedrzejas, 2000a), especially in the region of its polar head.

The inhibition of PLY by these sterols was investigated using a hemolytic assay (Walker et al., 1987), the results of which are summarized in Table 1. Derivatization of PLY with TNB abolished its measurable activity. Twenty-five percent of WT activity could be restored by the addition of DTT. The sterols in this assay were solubilized in 10% (v/v) ethanol (EtOH). Neither EtOH nor EtOH plus cholesterol lysed red blood cells. The activity of PLY was unaffected by EtOH but was completely abolished by cholesterol. Ergosterol reduced the toxin activity by 50%, whereas lanosterol was a completely ineffective inhibitor.

The functional stoichiometry of the cholesterol-PLY complex is 1:1

A series of samples with molar ratios of cholesterol/PLY ranging from 0.01 to 200 was prepared and incubated for 30 min at 37°C. The activity of the toxin in the different solutions was monitored using a hemolytic assay (described in Materials and Methods). In control fluorescence experiments we titrated PBS buffer with cholesterol so that the final concentration of sterol was sufficient to give an increase in light scattering signal (during fluorescence experiments, data not shown) providing evidence of micelle (or cholesterol aggregate) formation. All subsequent protein titration experiments with cholesterol were performed under conditions for which light scattering was negligible. We therefore assume that cholesterol was largely monomeric in our studies. Fig. 2 shows the toxin normalized activity (normalized HU) as a function of cholesterol/PLY molar ratio (hereafter, r) for

TABLE 1 Results from hemolytic assays with different sterol inhibitors of PLY activity

Buffer	PLY	PLY-TNB	DTT	EtOH	Chol	Ergo	Lano	% WT activity
×								NA
×	×							100
×		×						NA
×		×	×					25
×				×				NA
×				×	×			NA
×	×			×				100
×	×			×	×			NA
×	×			×		×		50
×	×			×			×	100

NA, no activity; Chol, cholesterol; Ergo, ergosterol; Lano, lanosterol.

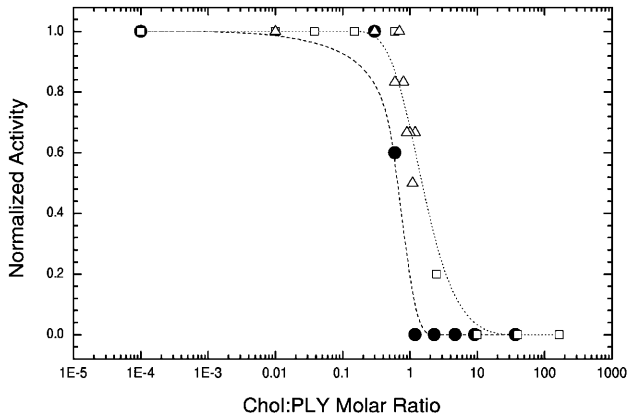

FIGURE 2 Normalized activity (normalized HU) of PLY as a function of the cholesterol/PLY molar ratio. A sharp transition in the toxin activity is seen when the molar concentration of cholesterol equals PLY molar concentration. The three symbols (and their corresponding *b*-spline interpolations) are triplicate measurements of the same data.

three parallel titrations. Each curve includes a sharp transition from full activity ($<r = 1$) to complete inhibition ($>r = 1$) implying that the functional stoichiometry of the cholesterol/PLY complex is 1:1.

Cholesterol/PLY binding and stoichiometry in solution

To investigate the binding of cholesterol to PLY in solution, the tryptophan (Trp) emission fluorescence was monitored as the cholesterol/PLY molar ratio was varied. PLY and cholesterol stock solutions were used as before. Trp fluorescence was excited at 290 nm and fluorescence emission spectra were measured between 300 and 650 nm. Fig. 3 shows typical Trp emission fluorescence spectra at different cholesterol/PLY molar ratios between 0:1 and 1:1. Six of the eight Trp residues in PLY are located in domain 4 (according to the homology model; Rossjohn et al., 1998). Of these, three are in the solvent-exposed Trp-rich loop, implicated in cholesterol-mediated membrane binding. Only one of the other three tryptophans in domain 4 is fully water-exposed. The seventh Trp in PLY forms part of an α-helix at the base of domain 3 and the eighth is positioned at the top of domain 1, although neither of these tryptophans is solvent-exposed in the model. The fluorescence maximum in Fig. 3 at 350 nm suggests that the fluorescence is mainly produced by Trp residues in a polar environment (see Vivian and Callis, 2001), and thus can be mostly attributed to the Trp residues in the Trp-rich loop, whereas fluorescence from buried tryptophans would have a maximum closer to 320 nm. The significant blue shift (10 nm) in the fluorescence maximum resultant upon an increase in cholesterol concentration implies that the Trp environment becomes more nonpolar upon addition of cholesterol, consistent with its binding to the sterol.

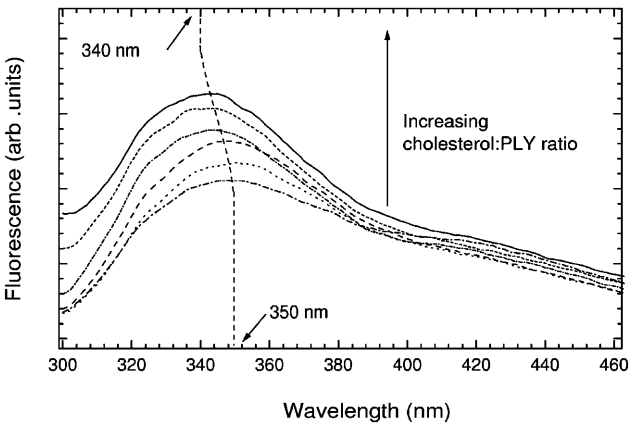

FIGURE 3 Typical tryptophan emission fluorescence spectra as the cholesterol/PLY molar ratio increases from 0:1 to 1:1.

Fig. 4 shows the change in normalized Trp fluorescence emission at 350 nm as the molar concentration of cholesterol increases. The increase in fluorescence emission indicates again that the Trp environment becomes more nonpolar. From the binding curve, it is possible to establish that the stoichiometry of the cholesterol/PLY complex is 1:1, in agreement with the functional stoichiometry measured via hemolytic assay (above). The dissociation binding constant (K_d) for the cholesterol/PLY complex was estimated to be 400 ± 100 nM by fitting a one-binding-site model to the data ($y = Bx/K_d + x$, where y is the normalized fluorescence, x is the molar cholesterol concentration, and B a normalizing constant). As a control for this study, PLY was titrated with ethanol (using the same injection volumes as with cholesterol): no change in the Trp fluorescence emission was observed; titration of PBS buffer with cholesterol under the same experimental conditions showed no fluorescence

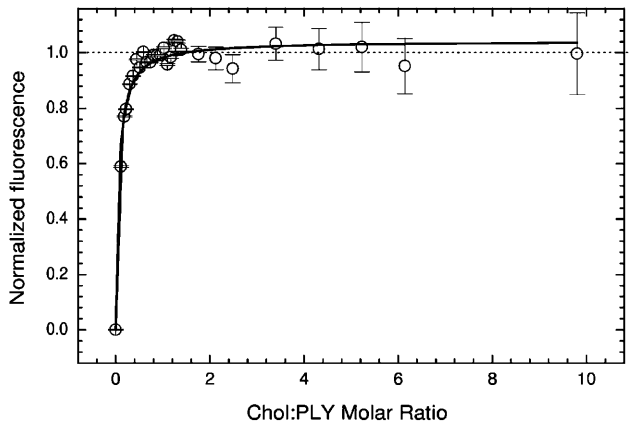

FIGURE 4 Tryptophan emission fluorescence at 350 nm as a function of cholesterol/PLY molar ratio. Cholesterol-binding saturation is reached at a cholesterol/PLY molar ratio of 1:1, and the estimated binding constant is 400 ± 100 nM. Solid line shows fit to the data using a one site-binding equation (see text for details).

signal. We conclude from these cholesterol titration experiments that cholesterol is able to bind to PLY in solution with an estimated binding constant of 400 ± 100 nM. In addition, the Trp emission fluorescence peak shows a blue shift indicating that the environment of the tryptophans involved in cholesterol binding becomes more nonpolar upon cholesterol binding.

Are there more cholesterol-binding motifs in PLY?

Ohno-Iwashita and colleagues determined that there are two cholesterol-containing binding sites for PFO in the membranes of sheep and human erythrocytes (Ohno-Iwashita et al., 1988), one with lower and the other with higher affinity. In our solution experiments we determined that the stoichiometry of the cholesterol-PLY complex in solution is 1:1. In the same experiments we estimated the binding constant to be 400 ± 100 nM, which is in agreement with the value measured previously by Ohno-Iwashita and colleagues for the low affinity binding site of PFO (Ohno-Iwashita et al., 1988) when bound to human erythrocytes. If different forms of cholesterol are bound by PFO and, by analogy, PLY, do these toxins therefore have more than one cholesterol-binding site? 21% of residues 126–354 of PLY are identical to the human-brain acid-soluble protein 1 (BASP1), also known as neuronal axonal membrane protein (NAP-22, GenBank accession number 6686256; Swissprot accession number P80723). The pairwise alignment between the two proteins shown in Fig. 5 reveals that NAP-22 is homologous with a large section of domain 1, 12 residues in domain 2, and all of domain 3 of PLY. These are mapped onto the homology model of PLY (based on PFO; Rossjohn et al., 1998) in Fig. 6. The alignment requires the introduction of only two single residue gaps in the NAP-22 sequence and the distribution of homology throughout the sequences is remarkably uniform. NAP-22 is a neuronal protein found localized on the inner leaflet of raft domains. Its ability to sequester cholesterol-rich domains is thought to be linked to its N-terminal myristoylation (Epand et al., 2001), although the myristoyl residue is probably more important for membrane insertion whereas the protein residues determine the interaction with cholesterol (Epand et al., 2002). The N-myristoylation sequence of NAP-22 (Fig. 5) overlaps with the cholesterol recognition/interaction sequence proposed by Terashita et al. (2002). Six of the 15 residues in PLY that align with this putative cholesterol recognition/interaction sequence are at least 90% identical with the corresponding NAP-22 sequence. Are there two cholesterol-binding/interaction motifs in PLY? Our tryptophan fluorescence data indicate the formation of a 1:1 stoichiometric complex between PLY and cholesterol, in apparent conflict with this hypothesis. However, these measurements were performed in solution: perhaps the two binding events are observed only upon interaction of PLY with membranes, as originally described by Ohno-Iwashita et al. (1988).

The second, putative cholesterol-binding motif described above overlaps with the epitope to which PLY-4, a monoclonal antibody capable of preventing oligomerization of PLY bound to cells, binds (Fig. 5). Does oligomerization of PLY, bound to cholesterol, drive the formation of lipid microdomains in cell membranes? Does this second binding motif recognize inner leaflet cholesterol (as in NAP-22) whereas the Trp-rich motif in domain 4 has a higher affinity for outer leaflet sterol? Little is known either about the mechanism through which NAP-22 sequesters cholesterol into domains or about the structure of the protein itself. It is not known whether NAP-22 self-associates either in the presence or absence of cholesterol. Although secondary

FIGURE 5 An alignment of the amino acid sequences of PLY and NAP-22 generated using MULTALIN (Corpet, 1988). The BLOSUM 62 matrix was used with a gap weight of 12 and a gap length weight of 2. Red indicates homology ≥90%; the symbol ''#'' is any one of NDQEBZ. The putative cholesterol-binding sequence is underlined. The approximate location of the PLY-4 epitope is represented by italics. Sequence numbering refers to the PLY sequence, as does the domain numbering. Two secondary structure predictions based on the programs PROF (http://www.aber.ac.uk/phiwww/prof/) and SAM (http://www.cse.ucsc.edu/research/compbio/sam.html) are shown for NAP-22. The PROF prediction for PLY is shown for comparison alongside the secondary structure of the high-resolution homology model (Fig. 6).

FIGURE 6 The homology model of PLY (Rossjohn et al., 1998) with the region spanning the NAP-22 homology shown in red. Residues ≥90% homology are shown in cyan; those corresponding to the four putative cholesterol-binding motifs are in purple. The cholesterol-binding toxin, conserved undecapeptide (to which cholesterol is thought to bind), is in green.

structure prediction programs predict that NAP-22 comprises either all random coil, or random coil plus helix, circular dichroism studies show that the protein contains ~50% β-structure (the rest being random coil apart from 7% helix; Epand et al., 2001). Neither the predicted nor the experimentally determined secondary structure of NAP-22 is homologous with the predicted secondary structure of PLY (Fig. 5). There are no proteins sufficiently homologous with NAP-22 for which a high-resolution structure has been determined. This precludes the prediction of a high-resolution structure for NAP-22. The secondary structure content of NAP-22 is insensitive to pH (between 7.4 and 4.5, close to the pI of the protein) and remains essentially unchanged upon addition of liposomes containing 40% cholesterol. This is not so for PLY if its mode of action is largely the same as for its homolog PFO, wherein monomer-monomer interactions drive two groups of three small α-helices in domain 3 to refold to form two β-hairpins upon membrane insertion (Shatursky et al., 1999; Hotze et al., 2002). However, such a refolding event might bring the putative second cholesterol-binding site into contact with the appropriate cholesterol receptor within the membrane.

Interestingly, Epand et al. (2001, 2002) based their identification of a putative cholesterol-binding motif on earlier work by Li and Papadopoulos (1998), who postulated a universal cholesterol-binding motif of the form -*L*/*V*-$(X)_{1-5}$-*Y*-$(X)_{1-5}$-*R*/*K*-. This motif occurs four times in PLY (residues 11–17, 144–152, 240–244, and 327–337; see Table 2 and Fig. 6), and in fact is not found in the position homologous with the putative cholesterol receptor in NAP-22. The four motifs are differentially conserved across the sequences of 16 cholesterol-binding toxins (Table 2), PLY being the only toxin in the list with all four motifs. PFO has two of the four motifs. In fact, a total of 17 such motifs can be identified in the list of 16 CBT sequences: some motifs are found only in one protein (e.g., *Motif 2* in Table 2 occurs in only one of the six sequences, PLY), whereas others are found in many (e.g., *Motif 1* in Table 2 occurs in nine of the 16 sequences).

The questions raised above have not been addressed in this article; instead, they have come to light during the course of our investigation on the mode of interaction of PLY with cholesterol. In future studies we hope to go some way toward exploring the possibility of additional cholesterol-binding motifs in PLY.

Neutron reflectivity experiments

Small-angle neutron scattering studies of the effect of PLY on model membranes, in the form of liposomes, have been described by Gilbert et al. (1999a). The liposome surface was shown to thicken after addition of PLY-TNB, which has been interpreted as being due to the binding of PLY-TNB monomers. By contrast, addition of WT PLY was shown to thin the liposomal surface, providing clear evidence of the pore-formation process that was taking place. The same thinning was observed upon addition of DTT to the sample containing liposomes and PLY-TNB, which accordingly confirmed that the thinning was due to pore formation. The authors proposed that changes in the structure of the membrane upon binding of monomeric PLY increase the efficiency of oligomerization—which, accordingly, triggers pore formation.

In this article we report a specular neutron reflectivity (NR) experiment performed to obtain additional information on the mechanism of interaction of PLY with model membranes. Specular reflectivity experiments are sensitive to the difference in neutron scattering density between regions of sample in the direction perpendicular to the surface of the sample, and therefore should be sensitive to changes in the structure of the bilayer due to the presence of the PLY. The wavelength of the cold neutrons used in the NR study (a few tenths of a nanometer) determines the length scales probed by the experiment. Typically NR is sensitive to structural features perpendicular to the plane of the sample

TABLE 2 Conservation of the four 4 putative cholesterol-binding motifs across 16 cholesterol-binding toxins

	Motif 1	Motif 2	Motif 3	Motif 4
S. pyogenes SLO	L..NY	LPARTQY	VSNVAYGR	YTSVFLK
S. equisimilis SLO	L..NY	LPARTQY	VSNVAYGR	YTSVFLK
S. canis SLO	L..NY	LPARTQY	VSNVAYGR	YTSVFLK
Alveolysin	L..NYNR	LPARLQY	VSNVAYGR	YTSVFLK
Tetanolysin	L..SYNR	LPARTQY	VSNVAYGR	YTTTFFK
Perfringolysin O	L..SYNR	LPARTQY	VSNVAYGR	YTSVFLK
Novyilisin	L..SYNR	LPARTQY	VSNVAYGR	YTSVFLK
Cereolysin	L..TY	LPARMQY	VSNVAYGR	YTSTFLK
Pneumolysin	LAMNYDK	VPARMQYEK	VAYGR	L..PISYTTSFLR
Intermedilysin	L..QYDK	VPARMQY	VSNVSYGR	V..PISYTTSFVK
Suilysin	L..TY	L....QY	VSSVSYGR	V..PISYSTNFVK
Listeriolysin O	L..DYNK	Y	VAYGR	V..PIAYTTNFLK
Seeligerilysin O	L..NYDK	Y	VAYGR	V..PISYTTNFLK
Ivanolysin O	L..DYDK	Y	VAYGR	V..PIAYTTNFLK
Pyolysin	L..KY	Y	VSYGR	V..PVSYAVNFLK
Septicolysin O	YTFVGR	—	—	LFFLVGYIVLRAK

SLO, Streptolysin O; —, signifies that the motif is completely absent.

with length scales ranging from a few Å to 500 Å. Neutrons are particularly suited to studying organic films because their penetration power is larger than, for example, x rays, and so they are able to provide data on buried interfaces.

Below the adsorbing block surface is a PFTE base block from which a section has been cut to act as a trough containing the liquid (in this case, solutions of liposomes). The neutrons enter through one of the block faces and are reflected from the silicon/liquid interface. If the difference in neutron scattering length density at successive interfaces is sufficient, the technique will be sensitive to the thickness and composition of the layers comprising the sample. First, the silicon-oxide layer was characterized by measuring the reflectivity profile of the silicon block with the three contrast-matched liquids (see Materials and Methods). Using a one-layer model, the thickness of the silicon oxide was found to be 8 ± 3 Å with a scattering length density (SLD) of 3.41×10^{-6} Å^{-2} and a roughness of 5 Å. This was then fixed for all the fits subsequently performed for the more complex reflectivity data.

We were interested in characterizing the main features of the bilayer and in particular, differences in the bilayer structure due to the presence of PLY. After characterization of the SiO_2 layer, a 2 mM SH liposome solution (~50 ml) was poured into the trough. Once in contact with the hydrophilic SiO_2 layer, the liposomes collapse and give rise to a unilamellar phospholipid bilayer. This bilayer was characterized by measuring the neutron reflectivity profiles at three contrasts. We fitted first the profiles with a one-layer model. At the three contrasts used (the case of D_2O is shown in Fig. 7) we measured the bilayer thickness to be 36 ± 5 Å, with an SLD that changes depending on the contrasts used. For the D_2O case shown in Fig. 7, the SLD of the layer was 2.12×10^{-6} Å^{-2}. This value is compatible with the value found by Johnson et al. (1991). The roughness of the layer was ≈6 Å. The values of the SLDs for the three contrast-matched liquids are consistent in all three cases with 30% of the liquids penetrating the bilayer, considering that the SLD of the bilayer is 0.2×10^{-6} Å^{-2}. This is compatible with findings of others (Charitat et al., 1999; Johnson et al., 1991). An 8 Å-thick layer of water was included in the fit with SLD depending on the percentage of D_2O in the buffer. We also performed a more refined fit to the data with a more complicated model to take into account the slightly different SLD of tail and head layers. Although we could obtain higher quality fits in some cases, these did not change the main results of our fits: the total thickness of the bilayer and the amount of water in it. To properly discern the different structures (water, tails, and heads) we will need to perform more experiments. The goal of our experiment was to determine the structure of the bilayer after the insertion of the toxin, so we have used a one-layer model for the bilayer in our fit (Fig. 8). When the bilayer contained deuterated cholesterol we observed that the total thickness of the bilayer was 42 ± 4 Å with a higher SLD owing to the deuteration.

Finally, the derivatized toxin was added with DTT (to a final concentration of 60 μg/ml) to the trough and the new reflectivity profiles were measured at the same contrasts as before (Fig. 7). Here the goal was to observe possible changes in the bilayer structure that may in turn give an insight into the penetration of the bilayer by the toxin. It is important to stress that we need to fit NR data using a model, and therefore some assumptions about the structure of the system have to be made. We have fitted the system using a two-layer model for the bilayer. The thicknesses were 22 Å and 20 Å, with a roughness of 7 Å, for the D_2O case with an SLD of 1.4×10^{-6} Å^{-2} for the first layer and 2.6×10^{-6} Å^{-2} for the second layer. The thicknesses of the layers were similar for the other contrasts. The calculated SLD of PLY (discounting exchange of protons for deuterons) is 3.25×10^{-6} Å^{-2}, thus we interpret the two layers as follows: the second (outer) layer has an elevated SLD because toxin has inserted into the

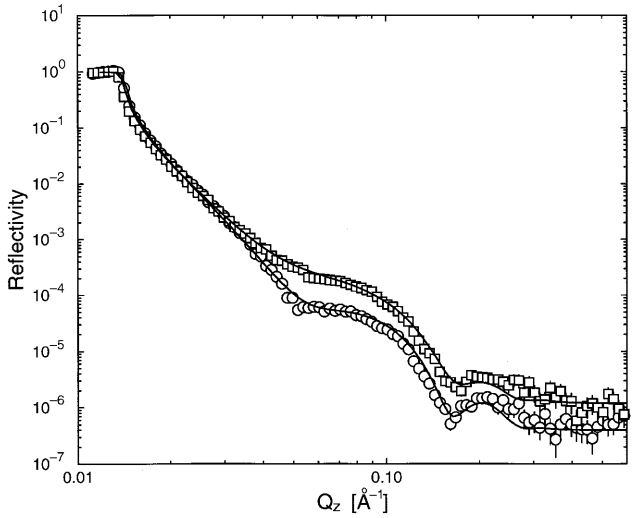

FIGURE 7 Neutron reflectivity curves for the bilayer adsorbed on the silicon in the presence (○) and absence (□) of activated toxin. Only the D_2O contrast is shown for clarity. The solid lines are the fits to a model described in the text.

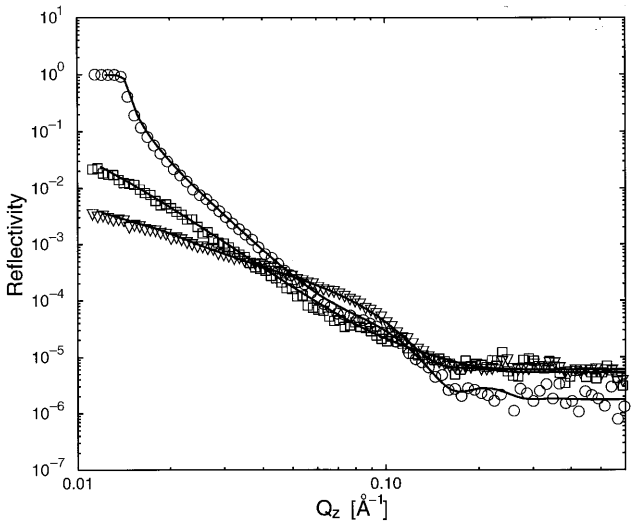

FIGURE 8 Neutron reflectivity profiles for the hydrogenated bilayer adsorbed onto the silicon-oxide substrate at the three contrasts: D_2O (○), H_2O (□), and 43% D_2O (▽). The profiles were fitted with a one-layer model for the bilayer for simplicity, as described in the text. The solid lines are fits to the data. A thin water layer was included on top of the silicon oxide during the fits, as observed by Charitat et al. (1999) and Johnson et al. (1991).

bilayer to a depth that corresponds to the thickness of this layer leaving the first (inner) layer free of toxin. Again, we stress that in the NR technique, a model must be used to fit the data, and we have considered the simplest one.

More experiments are needed to confirm these observations, and to further investigate the interaction of the toxin with bilayer, its level of penetration, and the formation of pores. Moreover, additional work is required to determine whether the deuterated cholesterol layer inside the lipid bilayer changes position after toxin insertion.

DISCUSSION

The main objective of this work was to study the interaction of cholesterol and PLY in solution. We determined the functional stoichiometry of the complex to be 1:1 by using a technique based on hemolytic assays. By the same means, we studied the specificity of the cholesterol-PLY interaction and demonstrated that sterols very similar to cholesterol are not able to efficiently inhibit PLY function. This implies that cholesterol perhaps cannot be replaced by other similar sterols to study its specific interaction with PLY, as was done in previous studies (Kelly and Jedrzejas, 2000a,b). Indeed Kelly and Jedrzejas observed saturation of ws-cholesterol binding to PLY at a PLY/ws-cholesterol molar ratio of ~1:3000, far in excess of the saturation point we have measured for standard cholesterol.

In addition, we employed tryptophan emission fluorescence spectroscopy to confirm the 1:1 stoichiometry of the cholesterol-PLY complex. In the same experiments we estimated the binding constant to be 400 ± 100 nM, in agreement with value measured previously by Ohno-Iwashita and colleagues for PFO (Ohno-Iwashita et al., 1988). That the tryptophan environment becomes more nonpolar upon binding cholesterol, reinforces the hypothesis that cholesterol interacts with PLY by specifically binding to the highly conserved Trp-rich loop. However, Ohno-Iwashita and colleagues determined that there are two cholesterol-containing binding sites for PFO in the membranes of sheep and human erythrocytes (Ohno-Iwashita et al., 1988). The high-affinity ($K_d \approx 2$ nM) site comprises ~3% of the total binding sites, whereas the majority have a 100-fold lower affinity ($K_d \approx 220$ nM). Are we measuring an average of these affinities for PLY? What is it about the binding sites for PFO that modulates the apparent binding affinity? Ohno-Iwashita et al. speculated that the accessibility of the toxin to the cholesterol in the high-affinity binding sites must not be restricted in the same way as for the low-affinity sites. Perhaps the high-affinity binding site is outer-leaflet cholesterol, whereas inner-leaflet cholesterol forms the low-affinity site—the asymmetry of the leaflets accounting for the difference in number of high- and low-affinity sites. Alternatively, the preferential localization of glycosphingolipids and sphingomyelin within the outer leaflet of lipid rafts could perturb access to cholesterol within raft domains: the high- and low-affinity sites may correspond to free and lipid-raft cholesterol, respectively. A further alternative model (Gilbert, 2002) ascribes the low-affinity binding site to cholesterol monomers dissolved in the membrane, whereas the high-affinity site is a tail-to-tail transbilayer cholesterol dimer. In the titration experiments reported here we observed essentially a low-affinity binding event, consistent with binding to cholesterol monomers.

Finally, we used neutron reflectivity to investigate the interaction of PLY with a phospholipid bilayer. PLY was shown to interact with the membrane by producing an effective change in the overall membrane thickness, by altering its neutron scattering length density and by forming a further layer of different scattering length density atop the phospholipid bilayer.

The authors thank Sean Langridge and Stephen Holt for assistance with neutron reflectivity studies on the CRISP and SURF instruments at ISIS.

The authors acknowledge support for neutron beam time from the Council for the Central Laboratory of the Research Councils (grants 11606 and 11607). Marcelo Nöllmann is the recipient of a Wellcome Trust Studentship.

REFERENCES

Alouf, J. E., and C. Geoffroy. 1991. The family of the antigenically related, cholesterol-binding (''sulphydryl-activated'') cytolytic toxins. *In* Sourcebook of Bacterial Protein Toxins. J. E. Alouf and J. H. Freer, editors. Academic Press, London, UK. 147–186.

Bonev, B. B., R. J. C. Gilbert, P. W. Andrew, O. Byron, and A. Watts. 2001. Structural analysis of the protein/lipid complexes associated with pore formation by the bacterial toxin pneumolysin. *J. Biol. Chem.* 276:5714–5719.

Byron, O., and R. J. C. Gilbert. 2000. Neutron scattering: good news for biotechnology. *Curr. Opin. Biotechnol.* 11:72–80.

Canvin, J. R., J. C. Paton, G. J. Boulnois, P. W. Andrew, and T. J. Mitchell. 1997. *Streptococcus pneumoniae* produces a second haemolysin that is distinct from pneumolysin. *Microb. Pathogen.* 22:129–132.

Charitat, T., E. Bellet-Amalric, G. Fragneto, and F. Graner. 1999. Adsorbed and free lipid bilayers at the solid-liquid interface. *Euro. Phys. J.* 8:583–593.

Corpet, F. 1988. Multiple sequence alignment with hierarchical clustering. *Nucleic Acids Res.* 16:10881–10890.

Duncan, J. L., and R. Schlegel. 1975. Effect of streptolysin O on erythrocyte membranes, liposomes, and lipid dispersions. A protein-cholesterol interaction. *J. Cell Biol.* 67:160–174.

Epand, R. F., S. Maekawa, and R. M. Epand. 2002. Structural requirements for the binding of the neuronal raft protein, NAP-22, to membranes. *Biophys. J.* 82:Meeting abstract 505d.

Epand, R. M., S. Maekawa, C. M. Yip, and R. F. Epand. 2001. Protein-induced formation of cholesterol-rich domains. *Biochemistry.* 40:10514–10521.

Gilbert, R. J. C. 2002. Pore-forming toxins. *Cell. Mol. Life Sci.* 59:832–844.

Gilbert, R. J. C., R. K. Heenan, P. A. Timmins, N. A. Gingles, T. J. Mitchell, A. J. Rowe, J. Rossjohn, M. W. Parker, P. W. Andrew, and O. Byron. 1999a. Studies on the structure and mechanism of a bacterial protein toxin by analytical ultracentrifugation and small-angle neutron scattering. *J. Mol. Biol.* 293:1145–1160.

Gilbert, R. J. C., J. L. Jiménez, S. Chen, I. J. Tickle, J. Rossjohn, M. Parker, P. W. Andrew, and H. R. Saibil. 1999b. Two structural transitions in membrane pore formation by pneumolysin, the pore-forming toxin of *Streptococcus pneumoniae*. *Cell.* 97:647–655.

Gilbert, R. J. C., J. Rossjohn, M. W. Parker, R. K. Tweten, P. J. Morgan, T. J. Mitchell, N. Errington, A. J. Rowe, P. W. Andrew, and O. Byron. 1998. Self-interaction of pneumolysin, the pore-forming protein toxin of *Streptococcus pneumoniae*. *J. Mol. Biol.* 284:1223–1237.

Heuck, A. P., E. M. Hotze, R. K. Tweten, and A. E. Johnson. 2000. Mechanism of membrane insertion of a multimeric β-barrel protein: perfringolysin O creates a pore using ordered and coupled conformational changes. *Mol. Cell.* 6:1233–1242.

Hotze, E. M., A. P. Heuck, D. M. Czajkowsky, Z. Shao, A. E. Johnson, and R. K. Tweten. 2002. Monomer-monomer interactions drive the prepore to pore conversion of a β-barrel-forming cholesterol-dependent cytolysin. *J. Biol. Chem.* 277:11597–11605.

Jacobs, T., M. D. Cima-Cabal, A. Darji, F. J. Méndez, F. Vázquez, A. A. C. Jacobs, Y. Shimada, Y. Ohno-Iwashita, S. Weiss, and J. R. de los Toyos. 1999. The conserved undecapeptide shared by thiol-activated cytolysins is involved in membrane binding. *FEBS Lett.* 459:463–466.

Jacobs, T., A. Darji, N. Frahm, M. Rohde, J. Wehland, T. Chakraborty, and S. Weiss. 1998. Listeriolysin O: cholesterol inhibits cytolysis but not binding to cellular membranes. *Mol. Microbiol.* 28:1081–1089.

Johnson, M. K., C. Geoffroy, and J. E. Alouf. 1980. Binding of cholesterol by sulfhydryl-activated cytolysins. *Infect. Immun.* 27:97–101.

Johnson, S. J., T. M. Bayerl, D. C. McDermott, G. W. Adam, A. R. Rennie, R. K. Thomas, and E. Sackmann. 1991. Structure of an adsorbed dimyristoylphosphatidylcholine bilayer measured with specular reflection of neutrons. *Biophys. J.* 59:289–294.

Kelly, S. J., and M. J. Jedrzejas. 2000a. Crystallisation and preliminary x-ray diffraction analysis of a functional form of pneumolysin, a virulence factor from *Streptococcus pneumoniae*. *Acta Crystallog.* D56:1452–1455.

Kelly, S. J., and M. J. Jedrzejas. 2000b. Structure and molecular mechanism of a functional form of pneumolysin: a cholesterol-dependent cytolysin from *Streptococcus pneumoniae*. *J. Struct. Biol.* 132:72–81.

Li, H., and V. Papadopoulos. 1998. Peripheral-type benzodiazepine receptor function in cholesterol transport. Identification of a putative cholesterol recognition/interaction amino acid sequence and consensus pattern. *Endocrinology.* 139:4991–4997.

Marsh, R. L., R. A. L. Jones, M. Sferrazza, and J. Penfold. 1999. Neutron reflectivity study of the adsorption of β-lactoglobulin at a hydrophilic solid/liquid interface. *J. Coll. Interf. Sci.* 218:347–349.

Morgan, P. J., P. W. Andrew, and T. J. Mitchell. 1996. Thiol-activated cytolysins. *Rev. Med. Microbiol.* 7:221–229.

Morgan, P. J., S. C. Hyman, O. Byron, P. W. Andrew, T. J. Mitchell, and A. J. Rowe. 1994. Modelling the bacterial protein toxin, pneumolysin, in its monomeric and oligomeric form. *J. Biol. Chem.* 269:25315–25320.

Morgan, P. J., S. C. Hyman, A. J. Rowe, T. J. Mitchell, P. W. Andrew, and H. R. Saibil. 1995. Subunit organisation and symmetry of pore-forming oligomeric pneumolysin. *FEBS Lett.* 371:77–80.

Nakamura, M., N. Sekino, M. Iwamoto, and Y. Ohno-Iwashita. 1995. Interaction of θ-toxin (perfringolysin O), a cholesterol-binding cytolysin, with liposomal membranes: change in the aromatic side chains upon binding and insertion. *Biochemistry.* 34:6513–6520.

Nishibori, T., H. B. Xiong, I. Kawamura, M. Arakawa, and M. Mitsuyama. 1996. Induction of cytokine gene expression by listeriolysin O and roles of macrophages and NK cells. *Infect. Immun.* 64:3188–3195.

Ohno-Iwashita, Y., M. Iwamoto, K. Mitsui, S. Ando, and Y. Nagai. 1988. Protease-nicked θ-toxin of *Clostridium perfringens*, a new membrane probe with no cytolytic effect, reveals two classes of cholesterol as toxin binding sites on sheep erythrocytes. *Eur. J. Biochem.* 176:95–101.

Palmer, M., P. Saweljew, I. Vulicevic, A. Valeva, M. Kehoe, and S. Bhakdi. 1996. Membrane-penetrating domain of streptolysin O identified by cysteine-scanning mutagenesis. *J. Biol. Chem.* 271:26664–26667.

Paton, J. C., P. W. Andrew, G. J. Boulnois, and T. J. Mitchell. 1993. Molecular analysis of the pathogenicity of *Streptococcus pneumoniae*—the role of pneumococcal proteins. *Annu. Rev. Microbiol.* 47:89–115.

Penfold, J. 1991. Instrumentation for neutron reflectivity. *Phys. B.* 173:1–10.

Penfold, J., R. C. Ward, and W. C. Williams. 1987. A time-of-flight neutron reflectometer for surface and interfacial studies. *J. Phys. E Scient. Instr.* 20:1411–1417.

Prigent, D., and J. E. Alouf. 1976. Interaction of streptolysin O with sterols. *Biochim. Biophys. Acta.* 443:288–300.

Ramachandran, R., A. P. Heuck, R. K. Tweten, and A. E. Johnson. 2002. Structural insights into the membrane-anchoring mechanism of a cholesterol-dependent cytolysin. *Nat. Struct. Biol.* 9:823–827.

Rossjohn, J., S. C. Feil, W. J. McKinstry, R. K. Tweten, and M. W. Parker. 1997. Structure of a cholesterol-binding, thiol-activated cytolysin and a model of its membrane form. *Cell.* 89:685–692.

Rossjohn, J., R. J. C. Gilbert, D. Crane, P. J. Morgan, T. J. Mitchell, A. J. Rowe, P. W. Andrew, J. C. Paton, R. K. Tweten, and M. W. Parker. 1998. The molecular mechanism of pneumolysin, a virulence factor from *Streptococcus pneumoniae*. *J. Mol. Biol.* 284:449–461.

Shatursky, O., A. P. Heuck, L. A. Shepard, J. Rossjohn, M. W. Parker, A. E. Johnson, and R. K. Tweten. 1999. The mechanism of membrane insertion for a cholesterol-dependent cytolysin: a novel paradigm for pore-forming toxins. *Cell.* 99:293–299.

Shepard, L. A., A. P. Heuck, B. D. Hamman, J. Rossjohn, M. W. Parker, K. R. Ryan, A. E. Johnson, and R. K. Tweten. 1998. Identification of a membrane-spanning domain of the thiol-activated pre-forming toxin *Clostridium perfringens* perfringolysin O: an α-helical to β-sheet transition identified by fluorescence spectroscopy. *Biochemistry*. 37: 14563–14574.

Sibelius, U., F. Rose, T. Chakraborty, A. Darji, J. Wehland, S. Weiss, W. Seeger, and F. Grimminger. 1996. Listeriolysin is a potent inducer of the phosphatidylinositol response and lipid mediator generation in human endothelial cells. *Infect. Immun.* 64:674–676.

Smyth, C. J., and J. L. Duncan. 1978. Thiol-activated (oxygen-labile) cytolysins. *In* Bacterial Toxins and Cell Membranes. J. Jeljaszewicz and T. Wadström, editors. Academic Press, London, New York, San Francisco. 129–183.

Terashita, A., N. Funatsu, M. Umeda, Y. Shimada, Y. Ohno-Iwashita, R. M. Epand, and S. Maekawa. 2002. Lipid binding activity of a neuron-specific protein NAP-22 studied in vivo and in vitro. *J. Neurosci. Res.* 70:172–179.

Tweten, R. K. 1995. Pore-forming toxins in Gram-positive bacteria. *In* Virulence Mechanism of Bacterial Pathogens. J. A. Roth, C. A. Bolin, K. A. Brogden, F. C. Minion, and M. J. Wannemuehler, editors. American Society for Microbiology, Washington, DC. 207–229.

Tweten, R. K., R. W. Harris, and P. J. Sims. 1991. Isolation of a tryptic fragment from *Clostridium perfringens* θ-toxin that contains sites for membrane binding and self-aggregation. *J. Biol. Chem.* 266:12449–12454.

Vivian, J. T., and P. R. Callis. 2001. Mechanisms of tryptophan fluorescence shifts in proteins. *Biophys. J.* 80:2093–2109.

Walker, J. A., R. L. Allen, P. Falmagne, M. K. Johnson, and G. J. Boulnois. 1987. Molecular cloning, characterisation, and complete nucleotide sequence of the gene For pneumolysin, the sulfhydryl-activated toxin of *Streptococcus pneumoniae*. *Infect. Immun.* 55:1184–1189.

Watson, K. C., T. P. Rose, and E. J. C. Kerr. 1972. Some factors influencing the effect of cholesterol on streptolysin O activity. *J. Clin. Pathol.* 25:885–891.

Yoshikawa, H., I. Kawamura, M. Fujita, H. Tsukada, M. Arakawa, and M. Mitsuyama. 1993. Membrane damage and interleukin-1 production in murine macrophages exposed to listeriolysin O. *Infect. Immun.* 61:1334–1339.